

# Yellow-red emitting, methoxy substituted triphenylamine-based styryl derivatives: Synthesis, photophysical properties, viscosity sensitivity, aggregation induced emission, NLO properties, and DFT study

Sulochana Bhalekar, Shantaram Kothavale, Nagaiyan Sekar\*

Department of Dyestuff Technology, Institute of Chemical Technology, Matunga, Mumbai, 400 019, India

## ARTICLE INFO

### Keywords:

Dicyanovinyltriphenylamine  
AIE  
ICT and TICT  
Viscosity sensitivity  
NLO

## ABSTRACT

Three novel triphenylamine based fluorescent molecular rotors (FMRs) are designed and synthesized to study the effect of auxiliary methoxy substituent on aggregation induced emission (AIE) and viscosity sensitivity. Instead of elongated, short conjugated dicyanovinyl derivatives are preferred for the improved AIE and viscosity sensitivity properties. The sensitivity study of fluorescence emission towards viscosity and polarity of organic solvents was investigated by UV visible solvatochromism study, while AIE study was performed in DMF-water mixture of solvents. All the compounds were well characterized by  $^1\text{H}$  and  $^{13}\text{C}$  NMR, mass spectra IR as well as elemental analysis. They exhibited very good solid state emission between 544–620 nm. High values for their first and second order hyperpolarizability ( $378\text{--}1755 \times 10^{-36}$  e.s.u) are observed. 'Two photon absorption cross sections' are in the range of 168–229 GM for 3. Effective charge transfer is elucidated using Mulliken Hush analysis.

## 1. Introduction

Due to its intramolecular charge transfer (ICT) ability triphenylamine based donor-acceptor organic compounds find applications in photovoltaic, dye sensitized solar cells (DSSCs) [1–5], 'organic light emitting diodes' (OLEDs) [6,7], 'organic thin field effect transistors' (OFETs) [8], sensors [9,10] and organic electronic devices [11]. Effective ICT for improved optoelectronic properties can be realized with the combination of strong donor and acceptor in the presence or absence of  $\pi$  bridge conjugation between donor and acceptor [12]. In general, donor- $\pi$ -acceptor compounds exhibit intramolecular or twisted intramolecular charge transfer (TICT). TICT is a dark state in which quenching of fluorescence takes place due to twisting of molecule in the excited state in polar solvents leading to the nonradiative relaxation with the bathochromic shift, and these molecules are referred to as Fluorescent Molecular Rotors (FMRs) [13]. It is always beneficial to synthesize FMRs which show enhancement of fluorescence in both micro and macro environment [14–16]. FMRs have biological applications like probes in vapor sensing [17], bioimaging [18] as biosensors [15].

Cyano group has been used in designing molecules optoelectronic devices because of its high polarizability and structural simplicity [19]. A combination of very good electron donating triphenylamine and

highly electron accepting cyano group creates AIEgens [20,21] with donor- $\pi$ -acceptor structures, which show very good solvatochromism, TICT, AIE as well as long wavelength emissions [20]. Recently, aggregation induced emissive dyes were extensively applied in OLEDs [22–26], solar cells [27], lasers [28], fluorescent probes [29], explosive detection, live cell bioimaging [30–32] and ion detection [33–36].

Triphenylamine based solid state emitters have wide applications in the field of OLEDs [37,38], DSSCs [39], lasers [40], nanoprobe for biomedical imaging [30], nanoparticles [41], Security printing, data storage and recording [42]. Solid state fluorescent compounds showing AIE property are of interest nowadays as they have wide applications in industries and research. [43]. Introduction of electron donating or accepting groups leads to alteration in molecular packing and decreases HOMO LUMO energy band gap are investigated to adopt solid state fluorescence [44].

Previously our group has reported triphenylamine styryl derivatives [45], as well as triphenylamine isophorone based styryl with methoxy as an auxiliary donor [13], which show viscosity sensitivity, ICT as well as TICT emission. But, extended conjugation can hinder their AIE as well as viscosity sensitivity properties [14,19]. Here, we synthesized mono (1), di (2) and tri (3) methoxy substituted triphenylamine based simple dicyanovinylene derivatives with decreased conjugation length. Three derivatives including D- $\pi$ -A (1) architecture with one methoxy as

\* Corresponding author.

E-mail address: [n.sekar@ictmumbai.edu.in](mailto:n.sekar@ictmumbai.edu.in) (N. Sekar).

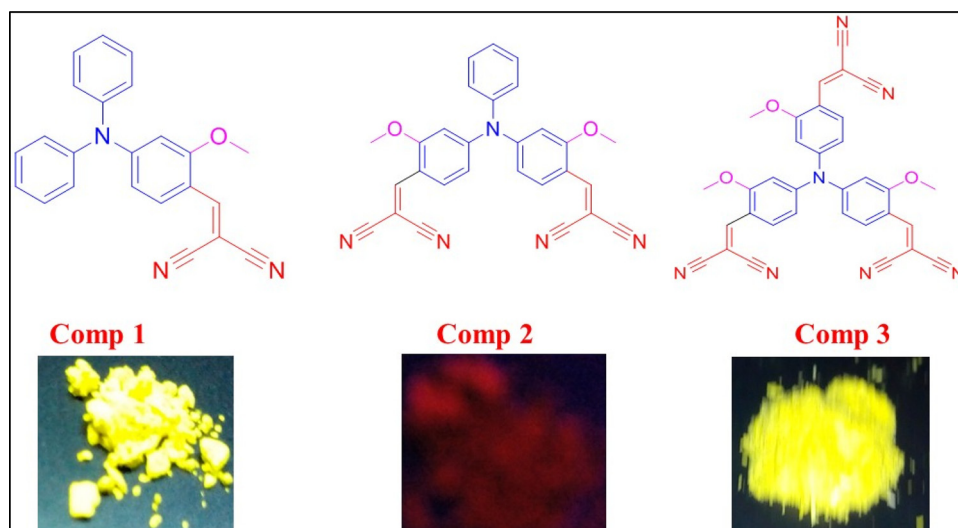


Fig. 1. Structure of the synthesized derivatives.

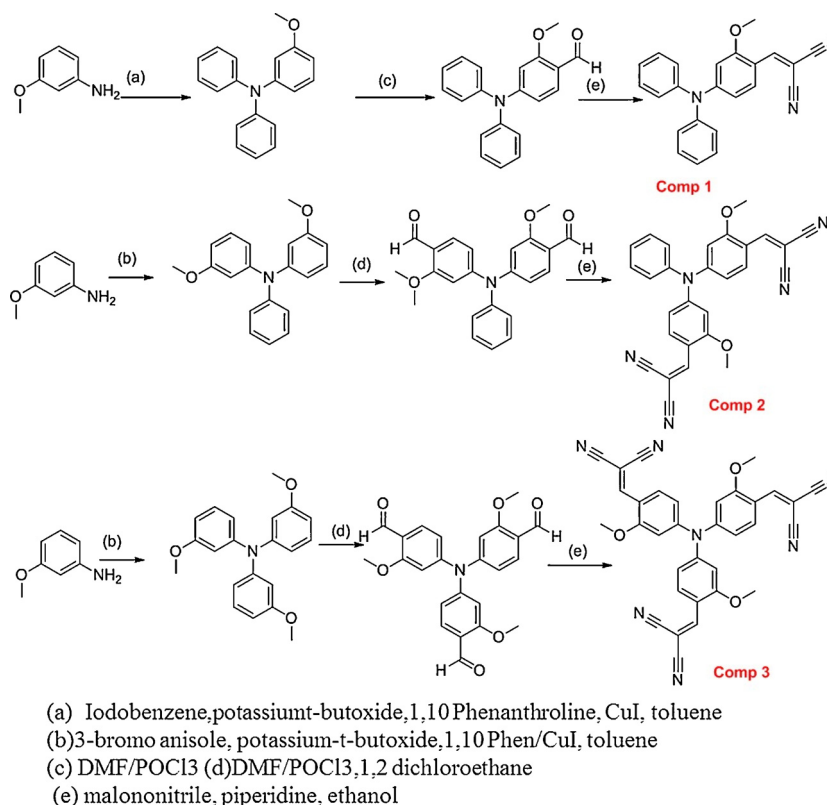


Fig. 2. Scheme 1. The synthetic route for compounds 1–3.

an auxiliary donor, A- $\pi$ -D- $\pi$ -A (2) with two methoxy auxiliary donors and A- $\pi$ -D- $\pi$ -A (3) with three methoxy auxiliary donors were designed to exhibit efficient FMR properties due to the freely rotating phenyl groups as well as rotating double bond of styryl unit. Additionally, as all the dyes show very good solid state fluorescence, enhanced AIE with the increasing percentage of water can be realized. All the dyes show quenching of fluorescence in polar solvents, but fluorescence enhancement in the viscous environment due to the hindering of free rotation of phenyl groups around C–N bond. All these dyes show very good solvatochromism, AIE, solid state fluorescence, and viscosity sensitivity and also high values of NLO properties compared to the three dyes without methoxy group [46] which leads to potential applications in the optoelectronic field as well as their capability to act as

NLOphores.

## 2. Materials and methods

Iodobenzene and potassium tertiary butoxide were purchased from Sigma Aldrich, India and remaining chemicals ordered from SD fine chemicals, Mumbai.  $^1\text{H}$  NMR and  $^{13}\text{C}$  NMR spectra were recorded on Agilent 500 MHz NMR.  $\text{CDCl}_3$ -d is used as solvent and Tetramethylsilane (TMS) as an internal standard. Fourier Transform infrared spectroscopy (FTIR) was performed on instrument SHIMADZU FTIR Japan 8400. Mass spectra are performed on Varian Inc USA, 410 Prostar Binary LC with 500 MS IT PDA detector in SAIF, IIT Bombay. The absorption spectra of the compounds were recorded on a Perkin

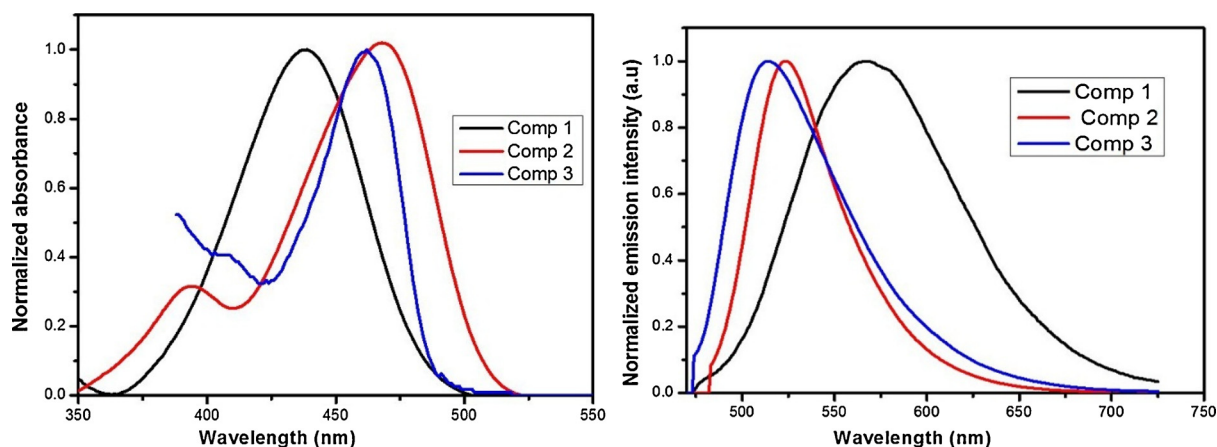


Fig. 3. Normalized absorption and emission graphs of all compounds in  $\text{CHCl}_3$  solvent.

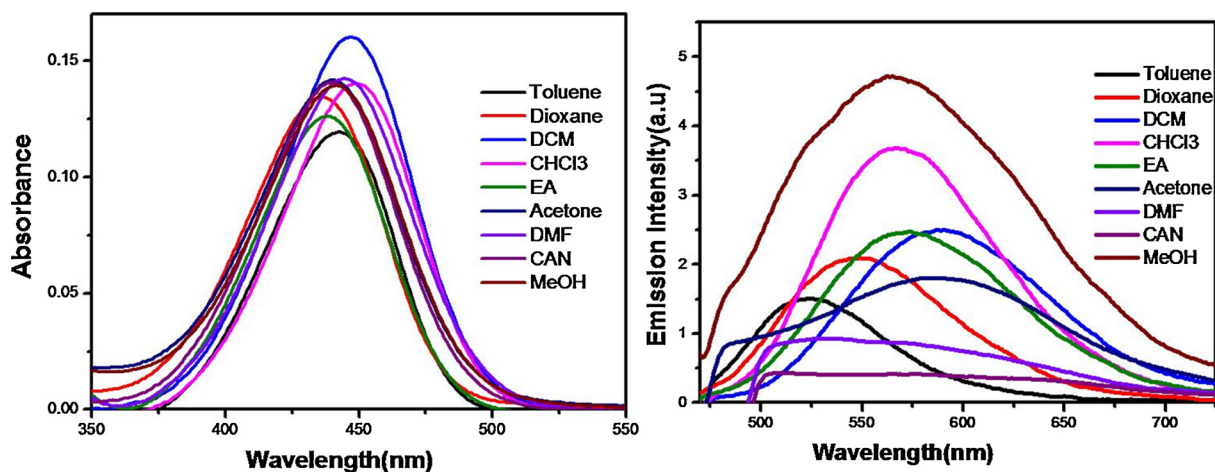


Fig. 4. Absorption and emission spectra of 1 in different organic solvents.

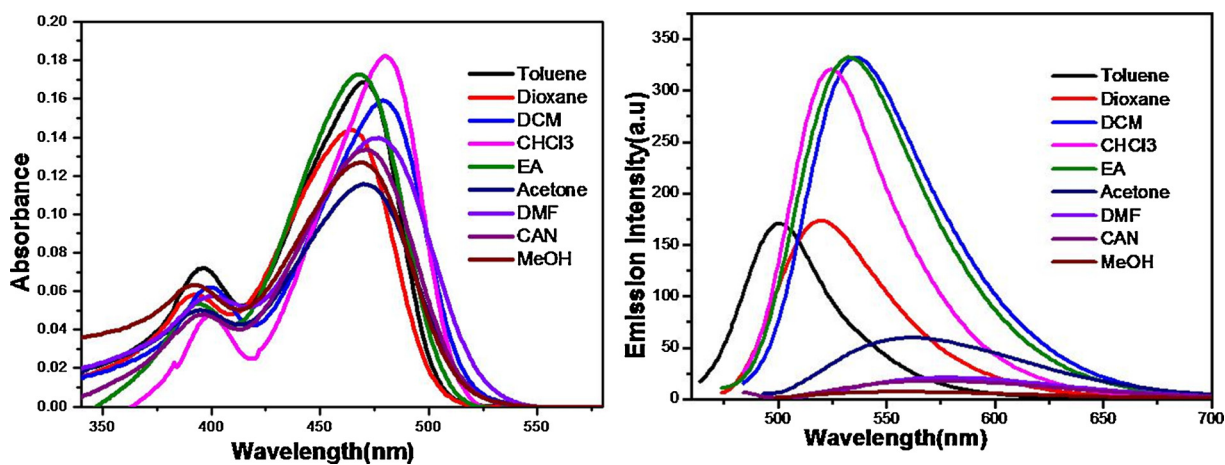


Fig. 5. Absorption and emission spectra of 2 in different organic solvents.

Elmer Lambda 25 UV-vis spectrophotometer; emission spectra were recorded on Varian Inc. Cary Eclipse spectrofluorometer. A concentration of  $2.5 \times 10^{-6} \text{ mol L}^{-1}$  was used in all the measurements. The quantum yield was calculated using coumarin 6 ( $\phi = 0.94$  in chloroform) as a reference standard by the relative quantum yield calculation method. DFT calculations were done by using Gaussian 09 software using 6-31g (d) basis set and the functionals, CAMB3LYP and BHandHLYP.

### 3. Experimental section

Mono, di, and tri methoxy triphenylamine styryl derivatives were synthesized from respective aldehydes by following the same procedure as given in the literature. The respective aldehydes were synthesized by following the same procedure reported by our group [13,47]

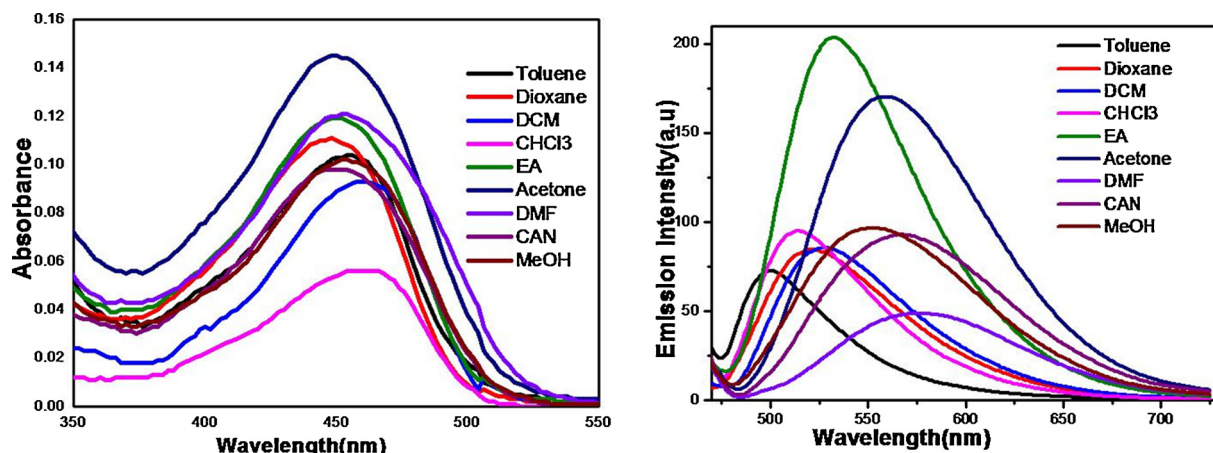


Fig. 6. Absorption and emission graphs of 3 in different organic solvents.

**Table 1**  
Photophysical parameters of 1.

Solvent	$\lambda_{\text{abs}}$	$\epsilon_{\text{max}} \times 10^4$	$\lambda_{\text{ems}}$	Stokes Shift		FWHM	$\phi_F$	$f$	$\mu_{\text{eg}}$	Kr	Knr	$\tau$
	nm	$\text{Lmol}^{-1}\text{cm}^{-1}$	nm	nm	cm <sup>-1</sup>							
Toluene	443	4.7	525	82	3525	61	0.010	0.77	8.55	3	2.89	0.03
Dioxane	436	5.4	548	112	4687	59	0.012	0.87	8.98	2.83	2.27	0.04
DCM	446	6.4	590	144	5472	59	0.016	0.89	9.23	2.59	1.56	0.06
Chloroform	449	5.6	567	118	4635	58	0.023	0.76	8.5	2.18	8.99	0.10
EA	439	5	573	134	5327	57	0.017	0.88	9.07	2.47	1.36	0.07
Acetone	440	5.7	587	147	5691	63	0.013	0.92	9.29	2.48	1.8	0.05
DMF	445	5.7	558	113	4550	61	0.009	1.04	9.92	2.64	2.64	0.03
Acetonitrile	440	5.6	581	141	5515	60	0.005	0.85	8.92	2.43	4.23	0.02
MeOH	442	5.6	562	120	4830	63	0.006	0.99	9.66	2.6	3.8	0.02

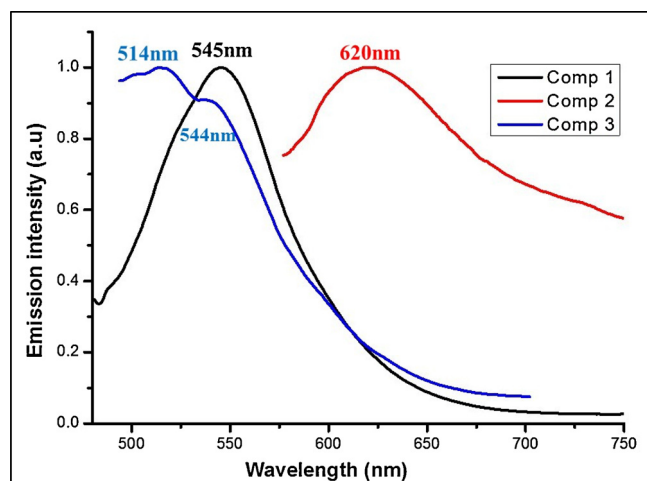


Fig. 7. Solid state emission graphs of all compounds.

### 3.1. (E)-2-(4-(Diphenylamino)-2-methoxybenzylidene) but-3-ynenitrile (1)-

To the solution of 4-(diphenylamino) 2-methoxybenzaldehyde (0.2 g, 6.6 mmol) and malononitrile (0.04 g, 6.8 mmol) in absolute ethanol 0.1 ml of piperidine were added. The mixture was refluxed for 1 h. On completion of the reaction, the reaction mixture was cooled to room temperature. Solid precipitated out was filtered and washed with a small amount of ethanol to isolate pure product as yellow solid. (0.2 g 78% yield, melting point: 194–196 °C)

<sup>1</sup>H NMR (500 MHz, cdCl<sub>3</sub>)  $\delta$  8.14 (d,  $J$  = 9.1 Hz, 1 H), 8.09 (s, 1 H), 7.39 (dd,  $J$  = 8.2, 7.6 Hz, 4 H), 7.27–7.19 (m, 6 H), 6.53 (dd,  $J$  = 9.1,

2.2 Hz, 1 H), 6.35 (d,  $J$  = 2.2 Hz, 1 H), 3.67 (s, 3 H).

<sup>13</sup>C NMR (126 MHz, CdCl<sub>3</sub>)  $\delta$  160.83, 155.43, 151.78, 145.09, 130.07, 129.88, 126.84, 126.16, 116.05, 114.79, 112.80, 111.88, 99.93, 73.39, 55.64.

Elemental analysis: Molecular formula- C<sub>23</sub>H<sub>17</sub>N<sub>3</sub>O; Expected C, 78.61 H, 4.88 N, 11.96. Obtained - C, 78.64 H, 4.87 N, 11.97.

Mass Data  $m/z$ -Expected 351.1372 obtained- $m/z$  +1-352.2

IR spectra (KBr Pellet) - 2214.13 (CN), 1589.23, 1564.16, 1490.87, 1352.01, 1303.79, 1232.43, 1159.14, 1122.49, 1027.99, 817.76, 757.97, 702.04.

### 3.2. 2,2'(((Phenylazanediy)bis(methoxy4,1phenylene))bis(methanylylidene))dimalononitrile(2)-

To the solution of (4,4'-(phenylazanediy) bis (2-methoxybenzaldehyde) (0.2 g, 5.54 mmol) and malononitrile (0.037 g, 6.65 mmol) in 10 ml absolute ethanol, 0.1 ml of piperidine was added. The mixture was refluxed for 1 h. On completion, reaction mixture was cooled to room temperature. Solid precipitated out was filtered and washed with small amount of ethanol to isolate pure product as red solid (0.18 g Yield: 75%, melting point: 198 °C)

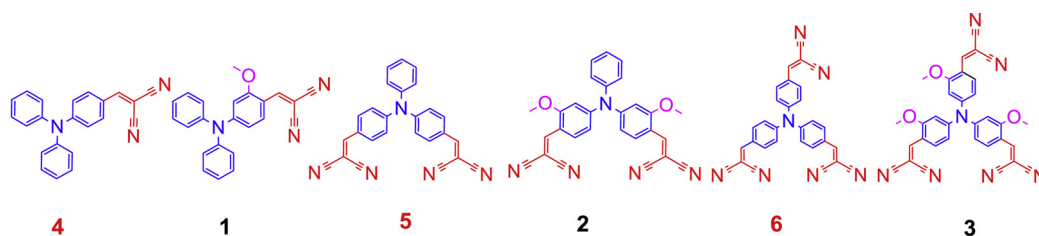
<sup>1</sup>H NMR (500 MHz, CdCl<sub>3</sub>)  $\delta$  8.20 (s, 1 H), 8.18 (s, 1 H), 8.15 (s, 1 H), 7.44 (t,  $J$  = 7.5 Hz, 2 H), 7.34 (t,  $J$  = 7.5 Hz, 1 H), 7.19 (d,  $J$  = 7.5 Hz, 2 H), 6.74 (d,  $J$  = 8.5 and 2 Hz, 1 H), 6.72 (d,  $J$  = 8.5, 2.0 Hz, 1 H), 6.59 (d,  $J$  = 2 Hz, 2 H), 3.74 (s, 6 H).

<sup>13</sup>C NMR (126 MHz, CdCl<sub>3</sub>)  $\delta$  160.34, 153.13, 152.08, 144.27, 130.36, 130.10, 127.42, 127.38, 115.75, 115.73, 115.00, 113.77, 104.93, 77.66, 55.96.

Elemental analysis- Molecular Formula- C<sub>28</sub>H<sub>19</sub>N<sub>5</sub>O<sub>2</sub>; Expected-C, 73.51 H, 4.19 N, 15.31, Obtained- C, 73.54 H, 4.18 N, 15.32.

Mass Data  $m/z$ -Expected 457.1539 obtained- $m/z$  +1-457.3

IR spectra (KBr Pellet) - 2217.98 (CN), 1589.23, 1560.66, 1487.01,



	Comp 1/4		Comp2/5		Comp3/6	
Solvent	Abs	Ems	Abs	Ems	Abs	Ems
Toluene	443/439	525/532	471/467	500/516	456/454	500/477
DCM	446/443	590/585	479/474	534/538	460/460	531/525
EA	439/431	573/572	468/461	532/538	450/450	532/526
CAN	440/432	581/574	477/462	571/569	454/454	566/559

Fig. 8. Comparative Absorption and emission of with and without methoxy styryl derivatives.

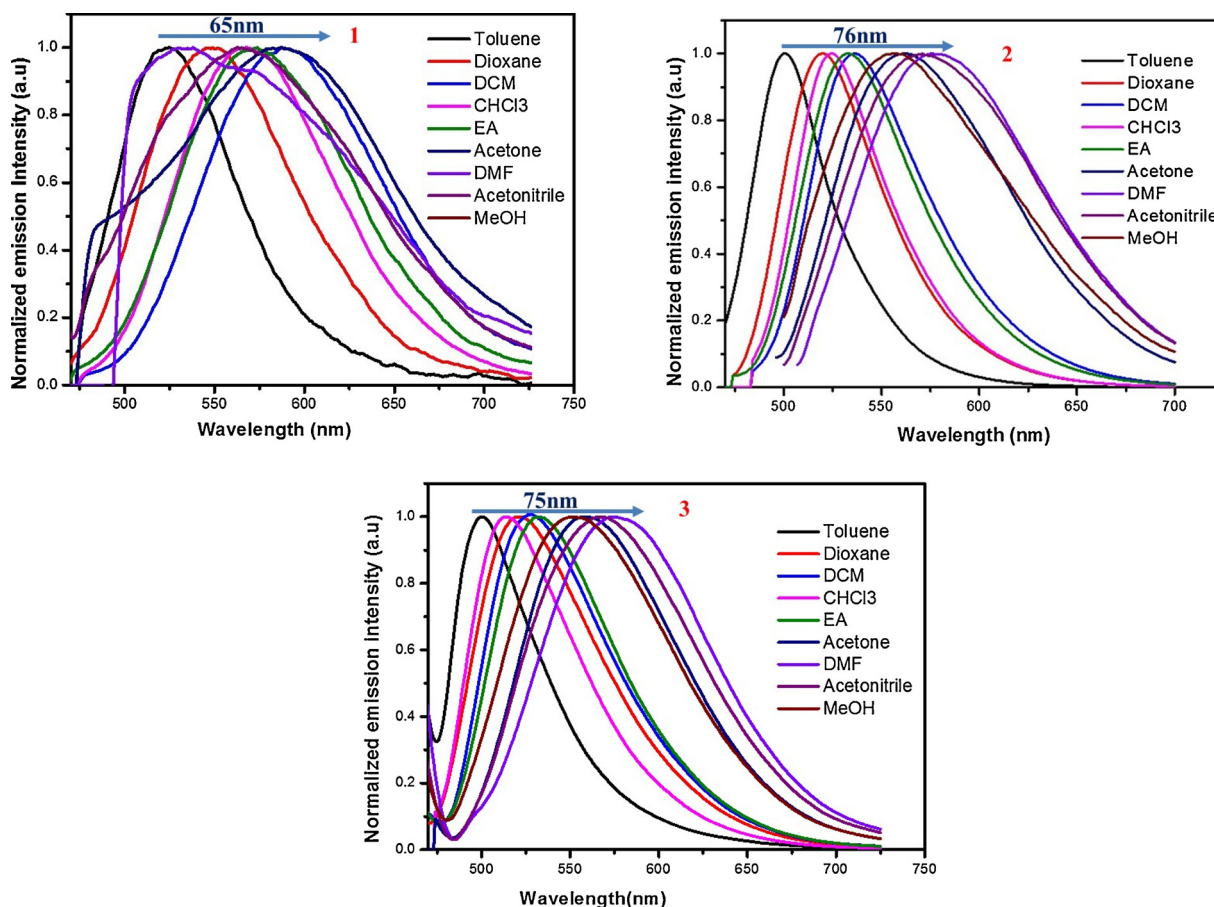


Fig. 9. Normalized absorption and emission spectra of all compounds.

1336.58, 1278.72, 1220.86, 1157.21, 1118.64, 1026.06, 918.05, 840.91, 744.47, 692.40

### 3.3. 2,2',2''-((Nitrilotris(2-methoxybenzene-4,1diyl))tris(methanylylidene))trimalononitrile-(3)-

To the solution of 4, 4', 4''nitrilotris (2-methoxybenzaldehyde) (0.2 g, 4.47 mmol) and malononitrile (0.031 g, 5.57 mmol) in absolute ethanol and 0.1 ml of piperidine was added. The mixture was refluxed

for 1 h. On completion, the reaction mixture was cooled to room temperature, solid precipitated out was filtered and washed with small amount of ethanol to isolate pure product as red solid (0.2 g, Yield-65%, melting point:190 °C).

<sup>1</sup>H NMR (500 MHz, dmsO)  $\delta$  8.32 (d,  $J$  = 8.4 Hz, 2 H), 8.03 (dd,  $J$  = 6.4, 4.9 Hz, 2 H), 6.98 (s, 1 H), 6.92 (s, 1 H), 6.87 (d,  $J$  = 6.4 Hz, 2 H), 6.83 (d,  $J$  = 8.4 Hz, 2 H), 5.73 (s, 3 H), 3.78 (s 3 H), 3.47 (s, H).

<sup>13</sup>C NMR (201 MHz, DMSO-*d*<sub>6</sub>)  $\delta$  163.01, 160.71, 154.16, 154.03, 152.58, 152.18, 130.87, 130.13, 117.82, 117.25, 116.65, 115.52,

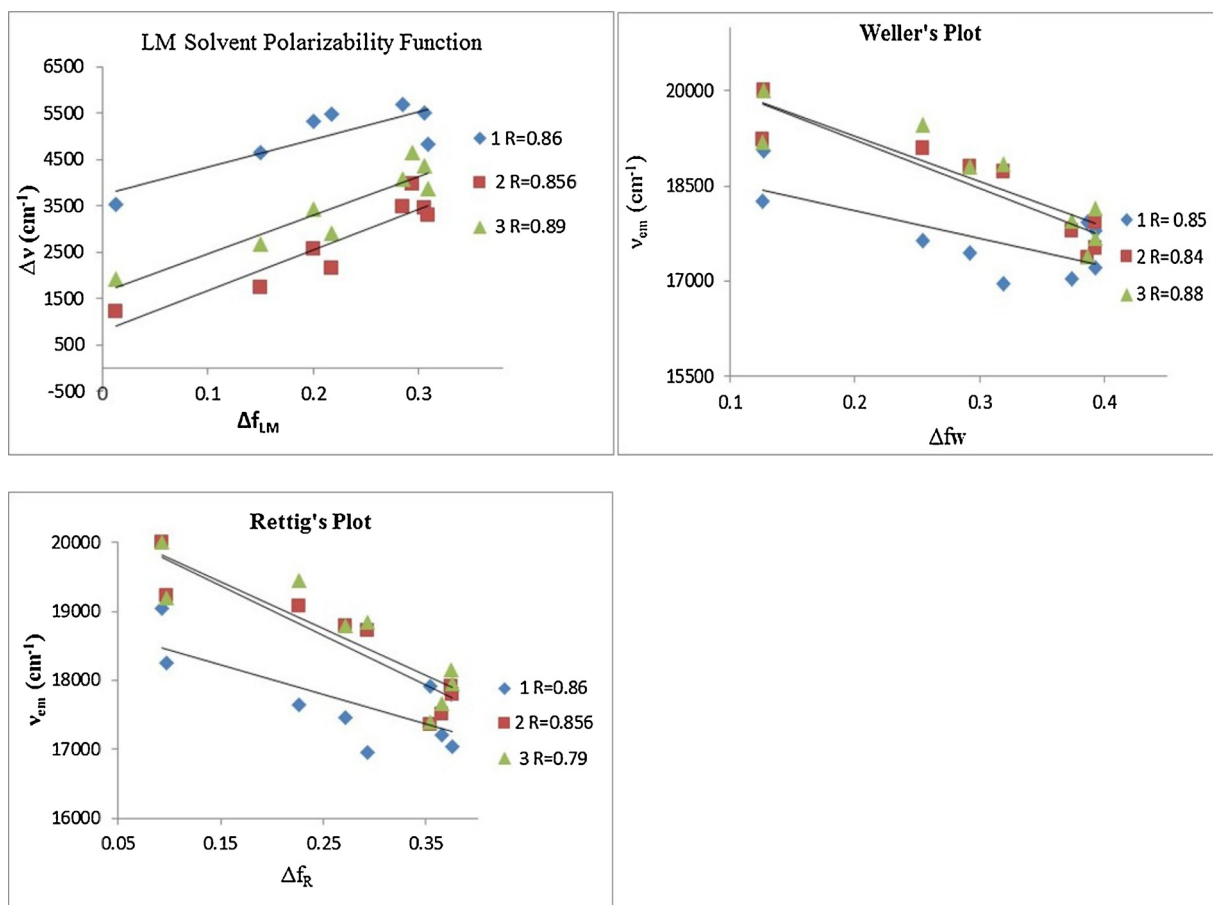


Fig. 10. Lippert Mataga, Weller and Rettig plot.

114.15, 108.12, 107.39, 78.48, 72.71, 70.20, 60.64, 56.87, 55.29 s.

Elemental analysis- Molecular Formula-  $C_{33}H_{21}N_7O_3$

Expected C, 70.33 H, 3.76 N, 17.40 Obtained- C, 70.34 H, 3.77 N, 17.41

Mass Data  $m/z$ -Expected 563.1706.1372 obtained- $m/z+1$  -564.1

IR spectra (KBr Pellet) - 2219.91 (CN), 1560.30, 1488.94, 1423.37, 1338.51, 1284.50, 1222.79 1064.63.792.69, 696.25. (Fig. 1 and 2)

#### 4. Photophysical properties

Photophysical properties including absorption  $\lambda_{max}$ , emission  $\lambda_{max}$ , molar extinction coefficient, and quantum yield for all the three compounds were studied in nine different organic solvents of variable polarities. The spectroscopic study was performed using  $2.5 \times 10^{-6}$  Mol  $L^{-1}$  concentration. They show absorption in 436–480 nm region and emission wavelength in 500–580 nm region, while Stokes shift from 29–147 nm and  $1231-5691\text{cm}^{-1}$  Fig. 3 represents the normalized absorption and emission graphs of **1**, **2**, and **3** in chloroform. For **2**, high energetic first shoulder peak was observed at 390 nm that can be assigned for the  $\pi-\pi^*$  transition while the low energetic main peak at 480 nm can be attributed to ICT peak from donating triphenylamine to acceptor dicyanovinyl group. [48] (Figs. 4–6)

Absorption wavelength,  $\lambda_{max}$  and molar extinction coefficient increase in the order of  $1 < 3 < 2$ . The compound **1** shows emission maximum at 525–590 nm, the compound **2** and **3** show emission maximum at 500–577 nm with quenching of fluorescence in polar solvents like DMF, acetonitrile, and methanol. Oscillator strength and transition dipole moment increase in the order  $1 < 2 < 3$  and the highest value of oscillator strength (1.79) and transition dipole moment (13.04) were observed for **3** in DMF which is due to the presence of

additional methoxy group. As a number of methoxy group increases the oscillator strength and transition dipole moment increase [49]. The nonradiative rate constant  $K_{nr}$  is higher than radiative rate constant  $K_r$ , which represents the TICT characters of the compounds. The fluorescence lifetime is measured using the equation S5 given in supporting information and it is very less for compound **1** (0.02–0.1 ns) while it is comparatively higher in dioxane for compound **2** and **3** (0.9 ns and 0.65 ns respectively). Table 1 represents all the photophysical properties of **1** in all the solvents using the equation S1–S5 given in supporting information. Table S1 and S2 represents all photophysical properties of **2** and **3**

All the three compounds exhibited very well solid state emission. The compound **1** shows emission maximum at 545 nm, the compound **2** shows emission maximum at 620 nm, and the compound **3** shows two emission maxima at 514 and 544 nm. All these emissions were obtained with the excitation at 450 nm wavelength. Fig. 7 represents the normalized graph of solid state emission.

We compared the absorption and emission of mono di and trisubstituted derivatives with and without methoxy group. compounds **1** and **3** show a bathochromic shift in absorption and emission intensity while compound **2** shows a red shift in absorption and slight blue shift in emission intensity around 4–16 nm shift compared to **5**. There is no measurable change in quantum yield. Synthesized derivatives show very good solid state emission, AIE property, viscosity sensitivity and also NLO properties. The comparative absorption and emission is given in Fig. 8

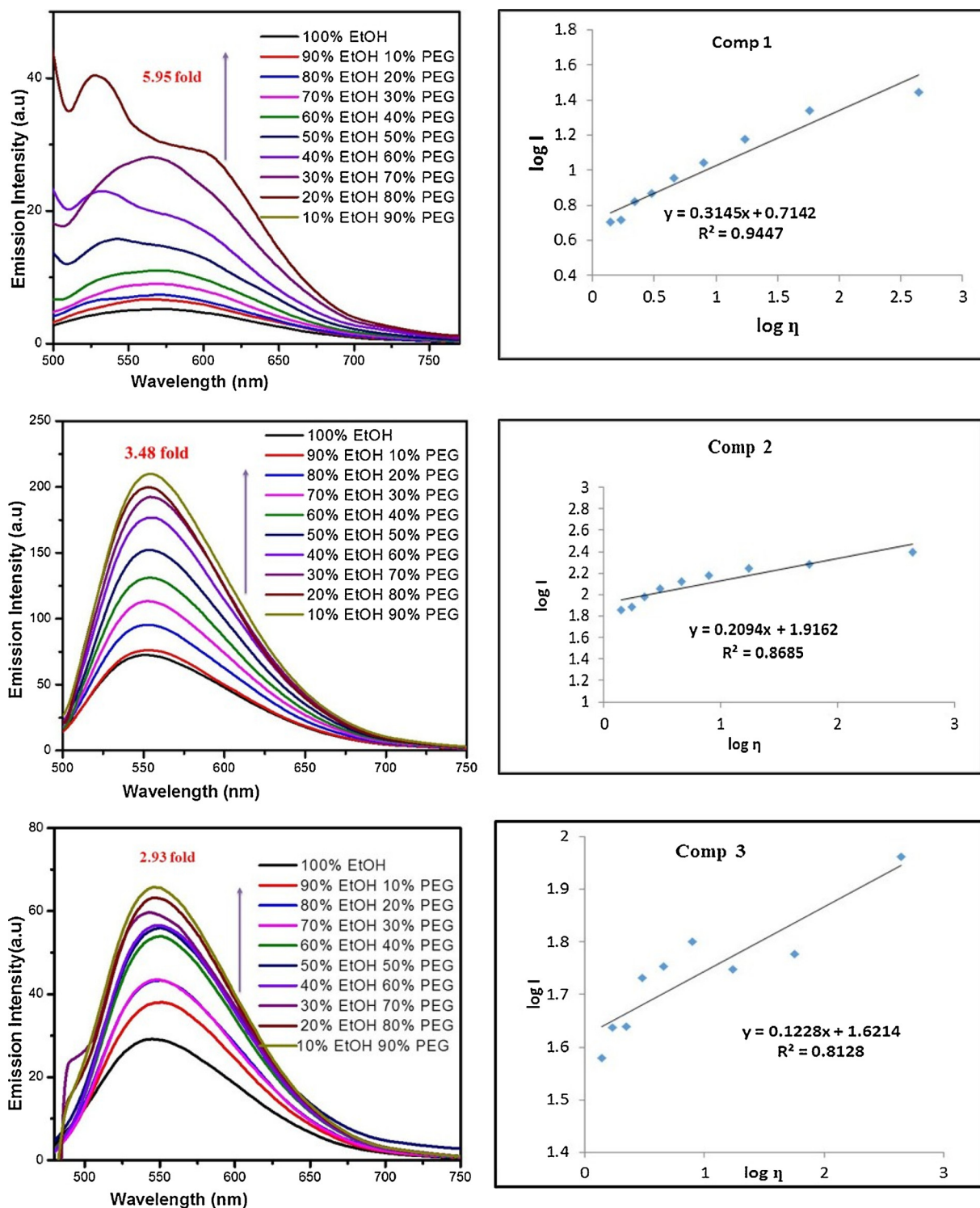


Fig. 11. Viscosity study of 1–3 in ethanol PEG 400.

#### 4.1. Solvatochromism, Lippert mataga correlation, and Solvent polarity function plots-

Fig. 9 represents the normalized emission spectra of 1, 2 and 3. All these compounds show 65–76 nm shift in emission from nonpolar to polar solvents. Hence to correlate the charge transfer, we have compared the Stokes shift versus Lippert Mataga function (orientation polarizability)  $f_1(\epsilon, n)$  and emission in  $\text{cm}^{-1}$  versus weller and Rettigs function in which the solvent dielectric constant and refractive index

are used. We have plotted Lippert Mataga [50] Weller and Rettig plot to check the solvatochromism in all the three compounds (Fig. 10) [51–54]. The equations for polarity functions are given in supporting information. All the compounds show regression constant around 0.8–0.9 for all functions which indicate effective charge transfer from donor to acceptor. Weller plot indicates the ICT character and Rettig's plot indicates TICT characteristics of these compounds. Further, to check whether compound shows TICT characteristics, we have done the viscosity study of all these compounds in PEG 400 and ethanol mixture

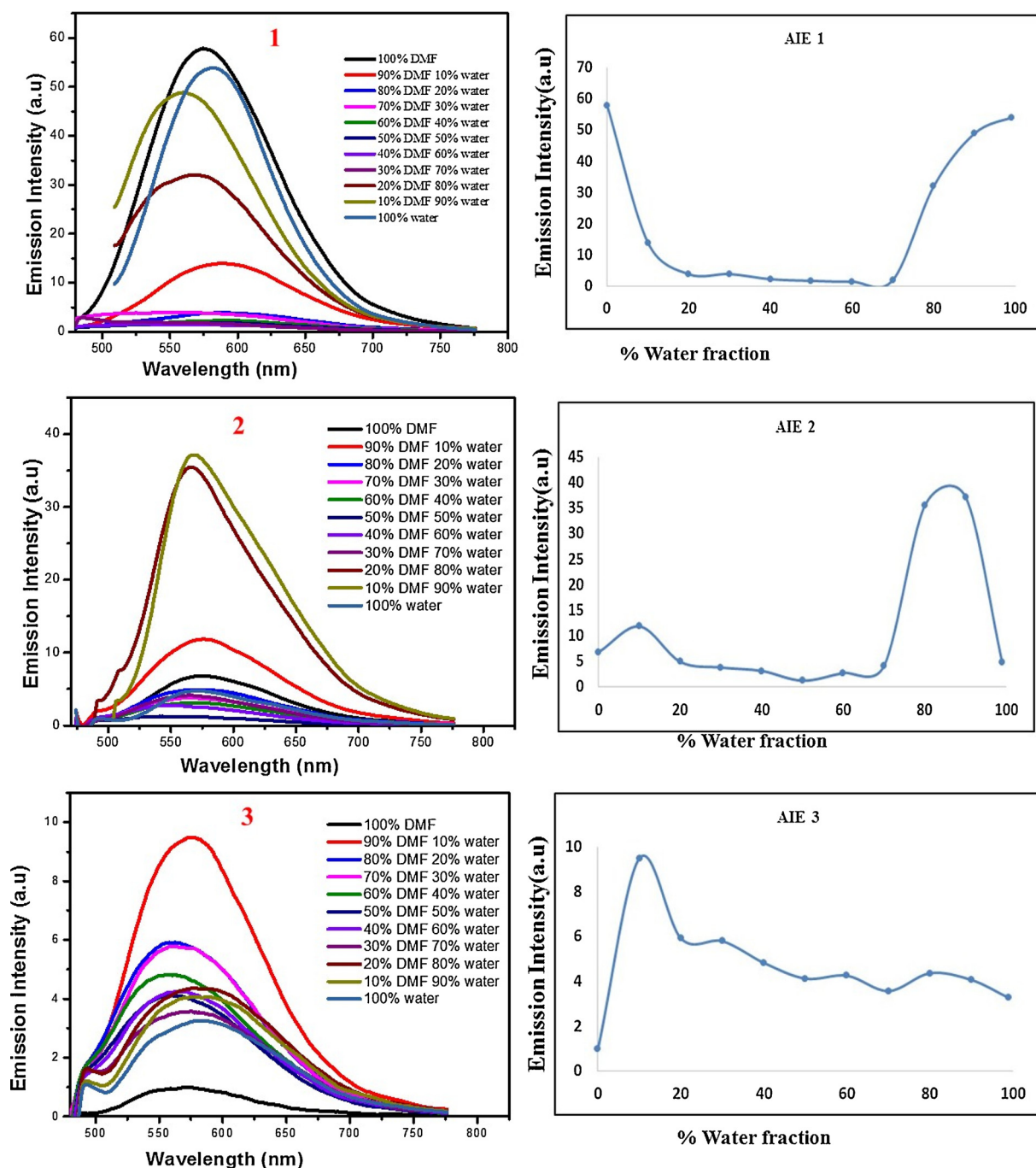


Fig. 12. Aggregation induced emission study of 1–3 in DMF water.

and found very good emission enhancement in a viscous environment.

#### 4.2. Viscosity study of 1, 2, 3 in PEG-Ethanol mixture

To study the microenvironment effect on these compounds, we carried the viscosity study of compounds in the mixture of viscous polyethylene glycol (PEG 400) and polar solvent, ethanol. It was observed that as we increase the percentage of PEG 400 in ethanol, emission intensity increases which are due to the restriction of rotation of freely rotating phenyl groups in a viscous environment. In the case of compound 1, the blue shifted band appears with an increasing percentage of PEG which could correspond to emission from the LE state and then dual emission is observed in the compound 1 which may be due to the transfer of an electron from LE and CT. Compounds 2 and 3

show a single emission with increasing the percentage of PEG 400. In the compounds 2 and 3, in polar solvents quenching of fluorescence takes place due to the TICT state. In viscous solvents, emission intensity increases with increasing viscosity due to the restriction of the TICT formation rate. The viscosity sensitivity of compounds is calculated using the Forster Hoffmann Eq. 6

$$\text{Log} I = C + x \log \eta \quad (1)$$

Where  $I$  is emission intensity,  $\eta$  is the viscosity of solvent  $C$  is constant  $x$  determines the sensitivity of compound.

1, 2 and 3 shows around 6, 3.5 and 3 fold increase in emission intensity respectively. (Fig. 11) Also from Forster Hoffman equation the constant and sensitivity obtained for 1, 2, 3 was ( $R_1 = 0.9$ ,  $X_1 = 0.31$ ) ( $R_2 = 0.8$ ,  $X_2 = 0.20$ ) and ( $R_3 = 0.8$ ,  $X_3 = 0.12$ ) respectively.

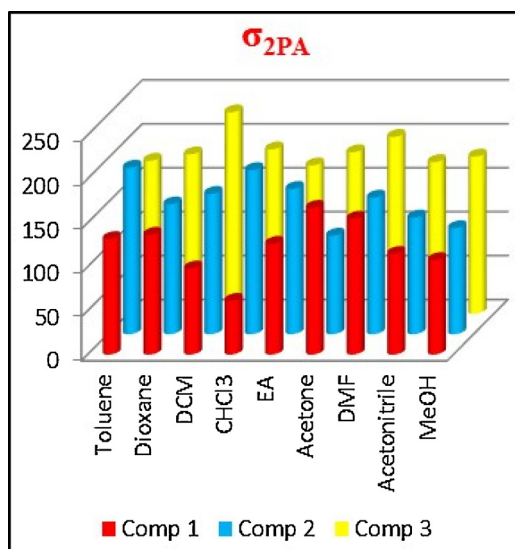


Fig. 13. Two photon absorption plot of -3.

#### 4.3. Aggregation induced emission enhancement (AIE) properties

The AIE characteristics of **1**, **2** and **3** were investigated in a mixture of DMF and water (Fig. 12). In DMF solvent, all the dyes show very weak emission in their solution states. To determine whether these dyes have AIE properties, the fluorescence spectra of dyes were measured in a series of DMF-water mixture. The concentration was maintained at  $2.5 \times 10^{-6}$  mol L<sup>-1</sup>. For **1** with the addition of water in a solution of DMF, the emission intensity was initially gradually decreased up to 30% DMF-70% water and then suddenly increased when 80% of water was added. The highest AIE enhancement was observed with 90% water in DMF. For **2** with the addition of water in a solution of DMF up to 70% emission intensity was decreased and at 80% water- 20% DMF again emission intensity was increased. In the case of **3**, emission intensity decreased with the increasing percentage of water suggesting concentration quenching (ACQ) mechanism.

#### 4.4. Two photon absorption? $\sigma_{\nu}^2$

Two photon absorption (TPA) is a nonlinear optical property which depends on structural configuration, ICT with a low HOMO-LUMO band gap of donor- $\pi$ -acceptor groups and shows higher values of  $\sigma_{\nu}^2$  [55]. TPA has applications in optical information storage, optical limiting and photodynamic therapy [56]. We calculated TPA values by using the equation given in reference [57]

$$\sigma_{\nu}^2 = \frac{12 \ln 10 \pi^3 L^4}{5 N_A h c^2 n^2} \left( \frac{\epsilon_{10(\nu)}}{\bar{\nu}_{10}} \right) \Delta \mu_{10}^2 \quad (2)$$

$$L = \left( \frac{2n^2 + 2}{3} \right)$$

where?  $\sigma_{\nu}^2$  is two photon absorption L is "Lorentzian local field factor,  $N_A$  is "Avogadro's number", h is "Planck's Constant", c is the "speed of light", n is the "refractive index" of solvent,  $\epsilon$  is the "molar extinction coefficient",  $\bar{\nu}_{10}$  is wavelength of absorption in cm<sup>-1</sup>.

Table 2

Two photon absorption values of compounds 1, 2, and 3.

Solvent $\Rightarrow$ Comp $\downarrow$	Toluene	Dioxane	DCM	CHCl <sub>3</sub>	EA	Acetone	DMF	ACN	MeOH
1	131.55	136.29	98.00	61.22	126.12	166.99	154.64	114.52	107.53
2	189.48	147.75	159.69	186.72	165.24	112.04	155.33	132.69	120.58
3	174.01	181.36	229.19	187.05	168.83	183.79	201.22	172.56	178.83

**1** shows TPA values around 61–166 GM. While **2** and **3** show comparatively higher values than **1**. As the band gap between HOMO and LUMO energy of **2** and **3** is low they show higher values of two photon absorption. Fig. 13 and Table 2 represents the two photon absorption values of all three compounds.

#### 4.5. "Generalized Mulliken-Hush analysis" for charge transfer

To correlate the charge transfer obtained by solvatochromic data we have calculated 'oscillator strength', transition dipole moment', the 'degree of delocalization' ( $C_b^2$ ) and 'strength of donor and acceptor' ( $H_{DA}$ ) and the 'distance between donor and acceptor' ( $R_{DA}$ ) for all compounds in toluene solvent using MH analysis [58,59].

'Oscillator strength' is calculated by using the equation

$$f = \frac{4.32 \times 10^{-9}}{n} \int \epsilon(\nu) d\nu$$

Where n is 'refractive index',  $\epsilon$  is 'molar extinction coefficient' and  $\int(\nu) d\nu$  is 'absorption coefficient area'.

'Degree of delocalization' is calculated by using the equation

$$C_b^2 = \frac{1}{2} \left( 1 - \sqrt{\frac{\Delta \mu_{ge}^2}{\mu_{ge}^2 + 4\mu_{ge}^2}} \right)$$

Where

$$\mu_{ge}^2 = \frac{3e^2 h}{8\pi^2 m c} \times \frac{f}{\nu_{eg}}$$

Where h is 'Planck's constant', m is 'mass of electron' e is 'charge on electron', c is 'speed of light' f is 'oscillator strength',  $\nu$  'frequency'.

Also 'electronic coupling matrix'  $H_{DA}$  is calculated using the equation

$$H_{DA} = \frac{\Delta E_{ge} \mu_{ge}}{\Delta \mu_{ab}}$$

Where?  $\mu_{ab}$  is 'difference in adiabatic dipole moment' and 'transition dipole moment',

$\Delta E_{ge}$  is 'vertical excitation energy'?  $\mu_{eg}$  is 'difference in dipole moment in the ground state and excite state'.

$$\Delta \mu_{ab} = \sqrt{\Delta \mu_{ge}^2 + 4\mu_{ge}^2}$$

Also 'distance between donor and acceptor'  $R_{DA}$  is calculated by using the equation

$$R_{DA} = 2.06 \times 10^{-2} \frac{\sqrt{\Delta E_{ge} \epsilon_{max} \Delta \nu_{1/2}}}{H_{DA}}$$

Where?  $\nu_{1/2}$  is 'band width'.

Values of  $C_b^2$  were found around zero (0.21-0.24) which shows a total degree of delocalization in the molecule and indicated effective ICT which is again correlated by using HOMO-LUMO energy band gap. Table 3 and Table S3. All these compounds show higher values of oscillator strength as well as transition dipole moment. Oscillator strength was found around 0.79–1.65 Debye. Compound **2** shows comparatively higher values of  $R_{DA}$  (3.63) and low value of  $H_{DA}$  (9070). Hence less the coupling constant matrix more is the charge separation between donor and acceptor, as they are inversely proportional to each other.

**Table 3**  
Mulliken hush analysis of all compounds in Toluene.

Comp	$a_0^a$ (Å)	$IAC^b$ ( $M^{-1} cm^{-1}$ )	$f^c$	$\Delta\mu_{CT}^d$ (Debye)	$\Delta\mu_{ge}^e$ (Debye)	$\Delta\mu_{ab}^f$ (Debye)	$Cb^{2g}$	$H_{DA}^h$	$R_{DA}^i$
									2.96
									3.63
3	6.5	3.74	1.64	15.17	12.62	29.44	0.24	9397	2.371

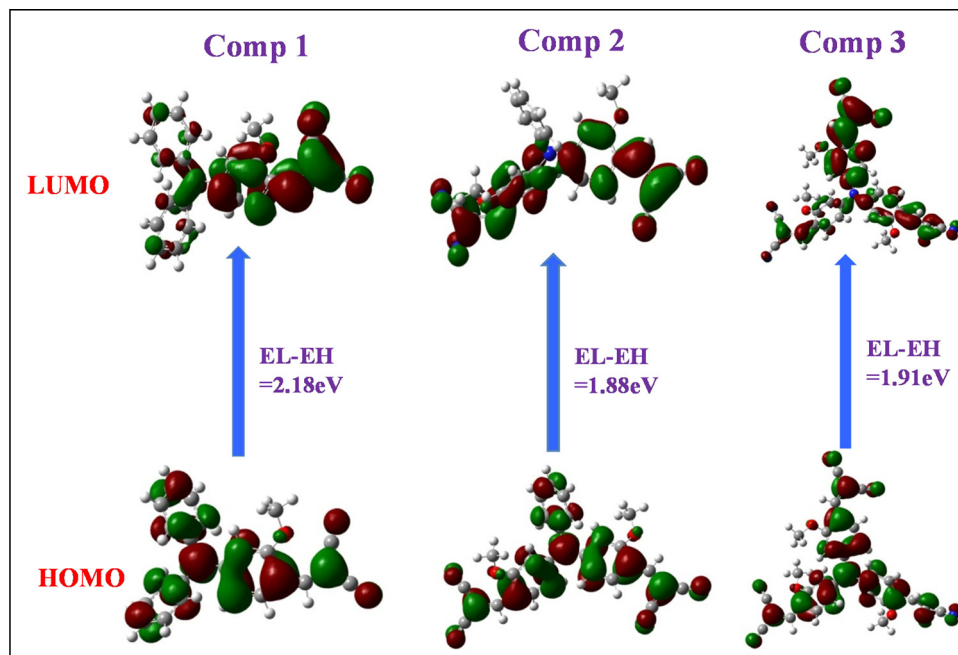


Fig. 14. Frontier Molecular orbital (FMO) diagrams with a band gap energy of all compounds.

**Table 4**  
Vertical excitation, Oscillator strength orbital contribution of all compounds in DMF.

Comp	$\lambda_{abs}^a$ nm	$\lambda_{abs}^b$ nm	$\lambda_{ems}^c$ nm	$f^{d1}$	$f^c$	$\mu_{eg}^f$	Major contribution
1	445	424	558	1.05	1.04	9.91	H → L 99.01
2	469	489	576	1.25	1.32	11.5	H → L 99.63
3	454	486	575	0.86	1.79	13.4	H → L 99.43

## 5. DFT computation

### 5.1. Optimization of structures by TD DFT method

We optimized the geometry of all the three compounds in the gas and solvent phase by using the 6-31 g (d) basis set with B3LYP functional [60–62]. Fig. 14 shows frontier molecular orbital (FMO) diagrams

**Table 5**  
Comparative values of Polarizability, First and second order hyperpolarizability in all solvents by the solvatochromic method.

Solvent	$\alpha \times 10^{-23}$			$\beta \times 10^{-30}$			$\gamma \times 10^{-36}$		
	1	2	3	1	2	3	1	2	3
Toluene	0.32	0.42	0.47	17	38.5	22	96	162.2	212.25
Dioxane	0.35	0.43	0.49	18.1	39.7	32.5	97	168.3	204.25
DCM	0.38	0.44	0.5	20.2	41.9	36.7	101.2	146.2	208.56
CHCl3	0.32	0.45	0.52	16.1	43.3	37.25	103.2	150.32	289.25
EA	0.36	0.49	0.55	18.9	46.7	35.4	107.5	170.25	347.25
Acetone	0.38	0.63	0.58	19.4	48.7	39.24	109.25	200.3	351.25
DMF	0.44	0.62	0.69	23.2	59	40.5	110.24	222.8	345.25
Acetonitrile	0.43	0.64	0.7	23.5	59.6	42.4	123.58	224.35	400.25
MeOH	0.42	0.67	0.72	22.4	59.7	42.56	120.25	238.25	421.25

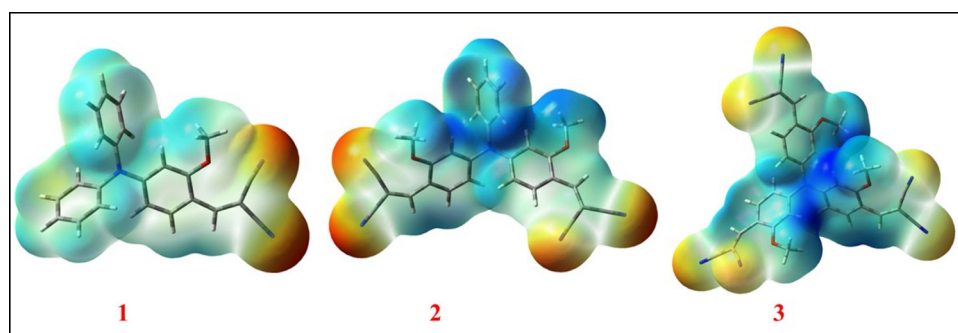
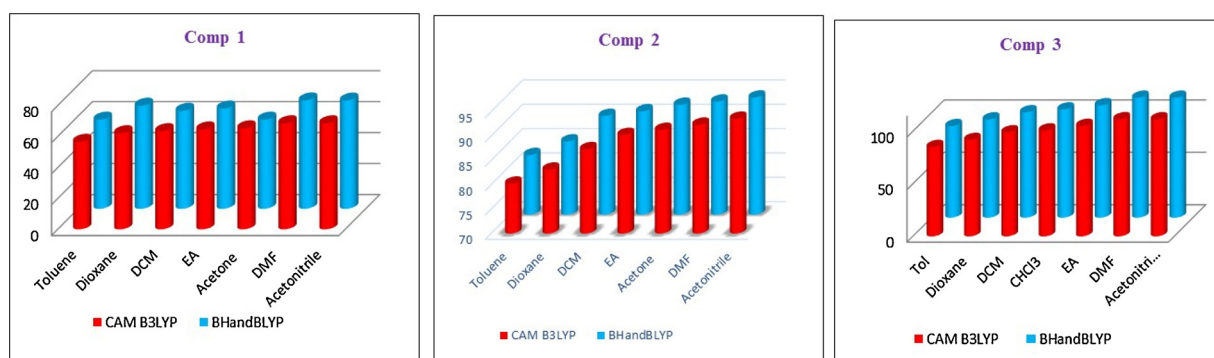
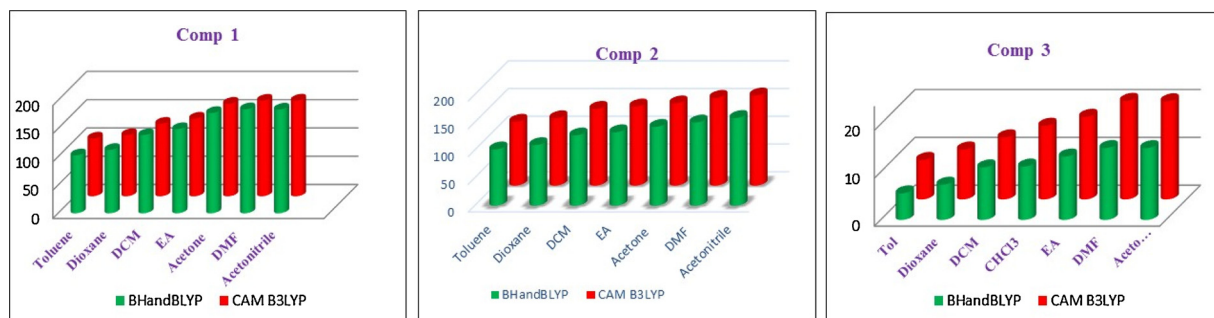
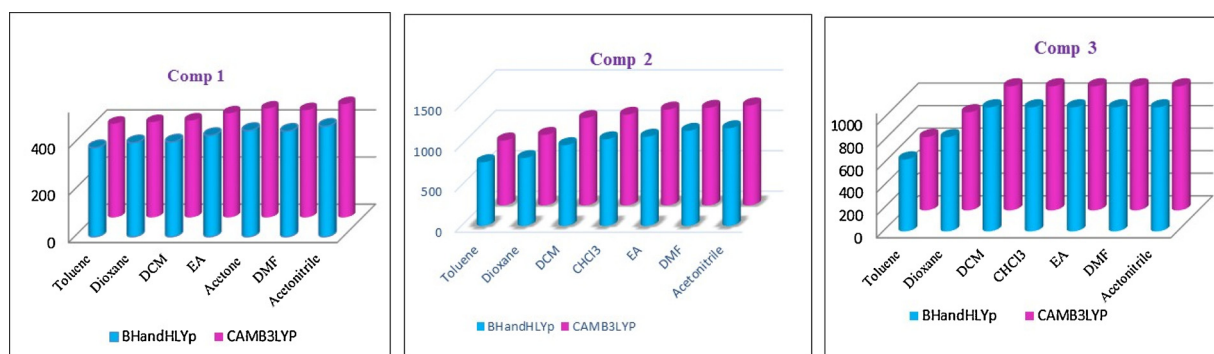


Fig. 15. MEP plots of compounds.

**Table 6**

Comparative values of dipole moment, Polarizability, First and second order hyperpolarizability in Toluene and DMF by DFT.

Comp	Functional	$(\mu)$ Debye		$(\alpha_0) \times 10^{-24}$ e.s.u		$\beta_0 \times 10^{-30}$ e.s.u		$\gamma \times 10^{-36}$ e.s.u	
		Toluene	DMF	Toluene	DMF	Toluene	DMF	Toluene	DMF
1	CAMB3LYP	13.77	16.29	57.55	69.99	102.58	184.06	398.25	456.07
	BHandHLYP	13.35	16.48	56.52	68.46	102.23	169.15	378.23	448.22
2	CAMB3LYP	12.07	14.75	82.25	93.24	115.25	158.36	802.14	1206.35
	BHandHLYP	12.23	14.70	80.25	92.35	101.67	150.25	787.25	1175.35
3	CAMB3LYP	6.001	7.83	87.36	114.46	8.25	20.6	838.5	1755.83
	BHandHLYP	6.1	8.00	85.25	111.69	5.56	15.04	830.38	1650.95

**Fig. 16.** Linear polarizability of 1–3 in solvents.**Fig. 17.** First order hyperpolarizability of 1–3 in solvents.**Fig. 18.** Second order hyperpolarizability of 1–3.

(HOMO and LUMO). From FMO diagrams it is noticed that HOMO is located on the entire structure while LUMO is mainly present on dicyano group in both 1 and 2 while in case of 3 HOMO is located on the entire structure while LUMO present only on two dicyanovinyl groups while third dicyanovinyl group remains vacant which suggest that it does not participate in the charge transfer process. In all three compounds, in their HOMO level oxygen present in the methoxy group also takes part in the charge transfer.

All the compounds show low band gap values (2.18 eV for 1, 1.88 eV for 2 and 1.91 eV for 3) which indicated an effective intramolecular charge transfer from donating triphenylamine and auxiliary methoxy to accepting cyano takes place. Particularly, 2 and 3 exhibited the lowest band gap than 1 indicating that with the increased number of acceptor unit as well as auxiliary methoxy donor charge transfer ability of these compounds was increased.

We have calculated oscillator strength  $f$ , major orbital contribution,

and vertical excitation. The values of experimentally observed absorption and oscillator strength for compounds 1 and 2 have the same trend as the theoretically obtained ones, and transition takes place from HOMO-LUMO with 99% orbital contribution. (Table 4), while for compound 3, the values obtained by DFT for oscillator strength is around 0.86 while experimentally observed values are around 0.55–1.79. Compound 2 shows comparatively higher value of absorption than 3 by both experimental and DFT methods which reveal that third dicyanovinyl group remains vacant which suggest that it does not participate in the charge transfer process which is clearly shown in the FMO diagrams hence compound 2 shows absorption at 469 and 489 by experimentally and by TD DFT respectively while 3 shows 454 and 486 respectively which shows a similar trend in observed values and DFT values.

Also, we have plotted ‘molecular electrostatic potential’ (MEP) plots to find the electrophilic and nucleophilic reactive sites of all three compounds. (Fig. 15) The electrophilic region is located on the dicyano group and the nucleophilic region is mainly located on nitrogen and phenyl rings.

## 6. Non linear optical properties

### 6.1. NLO properties by using Solvatochromism method

We have calculated the values for polarizability ( $\alpha$ ), first ( $\beta$ ) and second order hyperpolarizability ( $\gamma$ ) in different solvents [58,63,64]. All the equations for calculations of  $\alpha$ ,  $\beta$  and  $\gamma$  are given in the supporting information (Section 3 NLO properties by the solvatochromic method. All the three compounds show  $\alpha$ ,  $\beta$  and  $\gamma$  values of by several folds higher compared to urea. Table 5 represents all the values of  $\alpha$ ,  $\beta$  and  $\gamma$  in different solvents and all these values increase with increasing polarity. Table 6 reveals that all the compounds show an increase in the values of  $\alpha$ ,  $\beta$ , and  $\gamma$  with increasing polarity.

#### 6.1.1. NLO properties by using the DFT method

NLO properties in push pull chromophores are dependent on the effective intramolecular charge transfer from donor to acceptor from the ground state to excited state which attributed to higher values of linear polarizability and first order hyperpolarizability [65]. Polarizability and hyperpolarizability occur due to the strong polarizations between donor and acceptor in the presence of a strong electric field [66,67]. NLO materials have fast response time, low refractive index and dielectric constant, flexibility in structure and hence they have applications in optoelectronic and photonic devices [68]. We have calculated nonlinear optical properties like ‘dipole moment’ ( $\mu$ ), ‘linear polarizability’ ( $\alpha_0$ ), ‘polarizability anisotropy’ ( $\Delta\alpha$ ), ‘first order hyperpolarizability’ ( $\beta$ ) and ‘second order hyperpolarizability’ ( $\gamma$ ) by using functionals CAM B3LYP and BHandHLYP and 6-311+ g (d,p) basis set using the equations given below

dipole moment ( $\mu$ ) is calculated by using the equation

$$\mu = (\mu_x^2 + \mu_y^2 + \mu_z^2)^{1/2} \quad (3)$$

$$\alpha_0 = (1/3) [\alpha_{xx} + \alpha_{yy} + \alpha_{zz}] \quad (4)$$

$$\Delta\alpha = 2^{-1/2} [(\alpha_{xx} + \alpha_{yy})^2 + (\alpha_{zz} + \alpha_{xx})^2 + 6\alpha_{xx}^2] \quad (5)$$

$$(\beta_0) = (1/2) [\beta_x^2 + \beta_y^2 + \beta_z^2] \quad (6)$$

$$B_{\text{total}} = (1/2) [(\beta_{xxx} + \beta_{xyy} + \beta_{xzz})^2 + (\beta_{yyy} + \beta_{xxy} + \beta_{yzz})^2 + (\beta_{zzz} + \beta_{xxx} + \beta_{yyz})^2] \quad (7)$$

$$\gamma = (1/5) [(\gamma_{xxxx} + \gamma_{yyyy} + \gamma_{zzzz}) + 2(\gamma_{xxyy} + \gamma_{yyzz} + \gamma_{zzxx})] \quad (8)$$

Table 6 represents comparative values of dipole moment, polarizability, first and second order hyperpolarizability in toluene and DMF. Table S4 represents the NLO properties of all the three compounds in different solvents computed using CAMB3LYP and BHandHLYP functionals. 1 and 2 shows higher values of dipole moment (around 12–14

Debye) and first order hyperpolarizability (102–162  $\times 10^{-30}$  e.s.u. compared to 3 (dipole moment 6–8 Debye and  $\beta$  (5.56–20  $\times 10^{-30}$  e.s.u.). All the compounds show higher values of second order hyperpolarizability (378–1755  $\times 10^{-36}$  e.s.u.). 3 shows comparatively higher values of  $\gamma$  than 1 and 2. Also CAM B3LYP functional shows comparatively higher values for  $\alpha$ ,  $\beta$ , and  $\gamma$  than BHandHLYP functional in all the solvents for all three compounds. Figs. 16–18 indicates linear polarizability, first order hyperpolarizability and second order hyperpolarizability of 1, 2 and 3 respectively.

## 7. Conclusion

In this paper, we report methoxy supported triphenylamine based donor acceptor styryl dyes. Short conjugated malononitrile styryls were preferred over long conjugated styryls for effective viscosity sensitivity and AIE properties. They exhibited very good solvatochromism from non-polar to polar organic solvents which were supported by solvent polarity graphs. Viscosity sensitivity study in EtOH: PEG 400 mixture was carried out and found to show around 3 to 6 fold emission enhancement in all the three compounds, highlighting their capability to act as efficient FMRs. 1 and 2 show very good aggregation induced emission enhancement in DMF- water mixture and hence can be used in biological applications. FMO diagrams obtained by DFT method support effective intramolecular charge transfer (ICT) from HOMO to LUMO. All the experimental values are in good agreement with the theoretical values obtained from TD-DFT with major contribution 98–99 %. High values of their second order hyperpolarizability (378–1755  $\times 10^{-36}$  e.s.u) were obtained for all three compounds, hence they have the capability of showing good NLOphores properties.

## Acknowledgement

Author SBB and SK are thankful for University Grants Commission for JRF and SRF also we are thankful for SAIF department for mass analysis and TIFR for 13CNMR.

## Appendix A. Supplementary data

Supplementary material related to this article can be found, in the online version, at doi:<https://doi.org/10.1016/j.jphotochem.2019.112027>.

## References

- [1] S. Qu, J. Hua, H. Tian, New D- $\pi$ -A dyes for efficient dye-sensitized solar cells, *Sci. China Chem.* 55 (2012) 677–697, <https://doi.org/10.1007/s11426-012-4517-x>.
- [2] G. Tang, J. Zhou, W. Zhang, J. Hu, D. Peng, Q. Xie, C. Zhong, Novel D- $\pi$ -A dye sensitizers of polymeric metal complexes with triphenylamine derivatives as donor for dye-sensitized solar cells: synthesis, characterization and application, *Bull. Mater. Sci.* 38 (2015) 467–474, <https://doi.org/10.1007/s00289-014-1284-1>.
- [3] J.H. Yum, S.J. Moon, C.S. Karthikeyan, H. Wietasch, M. Thelakkat, S.M. Zakeeruddin, M.K. Nazeeruddin, M. Grätzel, Heteroleptic ruthenium complex containing substituted triphenylamine hole-transport unit as sensitizer for stable dye-sensitized solar cell, *Nano Energy* 1 (2012) 6–12, <https://doi.org/10.1016/j.nanoen.2011.08.004>.
- [4] Z. Tian, M. Huang, B. Zhao, H. Huang, X. Feng, Y. Nie, P. Shen, S. Tan, Low-cost dyes based on methylthiophene for high-performance dye-sensitized solar cells, *Dyes Pigm.* 87 (2010) 181–187, <https://doi.org/10.1016/j.dyepig.2010.03.029>.
- [5] A. Mahmood, Triphenylamine based dyes for dye sensitized solar cells: a review, *Sol. Energy* 123 (2016) 127–144, <https://doi.org/10.1016/j.solener.2015.11.015>.
- [6] X. Li, Y. Son, Y.S. Kim, S.H. Kim, J. Kun, J. Shin, Solvent dependent triphenylamine based D- $\pi$ -A type dye molecules and optical properties, *Nanosci. Nanotechnol.* 12 (2012) 1497–1502, <https://doi.org/10.1166/jnn.2012.4590>.
- [7] V.A. Online, J. Li, R. Wang, R. Yang, W. Zhou, X. Wang, Ligands : Color Tuning and Application in High- Performance Organic Light-emitting Diodes †, (2013), pp. 4171–4179, <https://doi.org/10.1039/c3tc30586d>.
- [8] S. Allard, M. Forster, B. Souharce, H. Thiem, U. Scherf, Organic semiconductors for solution-processable field-effect transistors (OFETs), *Angew. Chemie Int. Ed.* 47 (2008) 4070–4098, <https://doi.org/10.1002/anie.200701920>.
- [9] A. Kundu, S.P. Anthony, Triphenylamine based reactive coloro/fluorimetric chemosensors: structural isomerism and solvent dependent sensitivity and selectivity, *Spectrochim. Acta Part A Mol. Biomol. Spectrosc.* 189 (2018) 342–348, <https://doi.org/10.1016/j.saa.2018.08.004>.

- [org/10.1016/j.saa.2017.08.037](https://doi.org/10.1016/j.saa.2017.08.037).
- [10] S. Erdemir, S. Malkondou, A novel "turn on" fluorescent sensor based on hydroxy-triphenylamine for Zn<sup>2+</sup> and Cd<sup>2+</sup> ions in MeCN, *Sens. Actuators B Chem.* 188 (2013) 1225–1229, <https://doi.org/10.1016/j.snb.2013.08.031>.
- [11] Y.N. Luponosov, A.N. Solodukhin, S.A. Ponomarenko, Branched triphenylamine-based oligomers for organic electronics, *Polym. Sci. Ser. A Chem. Phys.* 56 (2014) 104–134, <https://doi.org/10.1134/S181123821401007X>.
- [12] Y. Sarigiannis, I.K. Spiliopoulos, Optical and electrochemical properties of poly-fluorenes with pyridine-triphenylamine bipolar unit, *Polym. Int.* 62 (2013) 196–203, <https://doi.org/10.1002/pi.4280>.
- [13] S. Kothavale, N. Sekar, Methoxy supported, deep red emitting mono, bis and tris triphenylamine-isophorone based styryl colorants: synthesis, photophysical properties, ICT, TICT emission and viscosity sensitivity, *Dyes Pigm.* 136 (2017) 116–130, <https://doi.org/10.1016/j.dyepig.2016.08.025>.
- [14] F. Zhou, J. Shao, Y. Yang, J. Zhao, H. Guo, X. Li, S. Ji, Z. Zhang, Molecular rotors as fluorescent viscosity sensors: molecular design, polarity sensitivity, dipole moments changes, screening solvents, and deactivation channel of the excited states, *Eur. J. Org. Chem.* (2011), <https://doi.org/10.1002/ejoc.201100606> n/a-n/a.
- [15] S.C. Lee, J. Heo, H.C. Woo, J.A. Lee, Y.H. Seo, C.L. Lee, S. Kim, O.P. Kwon, Fluorescent molecular rotors for viscosity sensors, *Chem. - A Eur. J.* 24 (2018) 13692, <https://doi.org/10.1002/chem.201803969>.
- [16] H. Yan, X. Meng, B. Li, S. Ge, Y. Lu, Design, synthesis and aggregation induced emission properties of two bichromophores with a triphenylamine-coumarin dyad structure, *Dyes Pigm.* 146 (2017) 479–490, <https://doi.org/10.1016/j.dyepig.2017.07.046>.
- [17] G. Martini, E. Martinelli, G. Ruggeri, G. Galli, A. Pucci, Julolidine fluorescent molecular rotors as vapour sensing probes in polystyrene films, *Dyes Pigm.* 113 (2015) 47–54, <https://doi.org/10.1016/j.dyepig.2014.07.025>.
- [18] M. Koenig, B. Storti, R. Bizzarri, D.M. Guldi, G. Brancato, G. Bottari, A fluorescent molecular rotor showing vapochromism, aggregation-induced emission, and environmental sensing in living cells, *J. Mater. Chem. C Mater. Opt. Electron. Devices* 4 (2016) 3018–3027, <https://doi.org/10.1039/C5TC03541D>.
- [19] J. Mei, N.L.C. Leung, R.T.K. Kwok, J.W.Y. Lam, B.Z. Tang, Aggregation-Induced Emission: Together We Shine, United We Soar!, *Chem. Rev.* 115 (2015) 11718–11940, <https://doi.org/10.1021/acs.chemrev.5b00263>.
- [20] S.-Y. Chen, Y.-W. Chiu, G.-S. Liou, Substituent effects of AIE-active  $\alpha$ -cyanostilbene-containing triphenylamine derivatives on electrofluorochromic behavior, *Nanoscale* 11 (2019) 8597–8603, <https://doi.org/10.1039/C9NR02692D>.
- [21] H.-T. Lin, C.-L. Huang, G.-S. Liou, Design, Synthesis, and Electrofluorochromism of New Triphenylamine Derivatives with AIE-Active Pendent Groups, *ACS Appl. Mater. Interfaces.* 11 (2019) 11684–11690, <https://doi.org/10.1021/acsami.9b00659>.
- [22] Z. Ning, Z. Chen, Q. Zhang, Y. Yan, S. Qian, Y. Cao, H. Tian, Aggregation-induced emission (AIE)-active starburst triarylamine fluorophores as potential non-doped red emitters for organic light-emitting diodes and Cl<sub>2</sub> gas chemodosimeter, *Adv. Funct. Mater.* 17 (2007) 3799–3807, <https://doi.org/10.1002/adfm.200700649>.
- [23] W.Z. Yuan, Y. Gong, S. Chen, X.Y. Shen, J.W.Y. Lam, P. Lu, Y. Lu, Z. Wang, R. Hu, N. Xie, H.S. Kwok, Y. Zhang, J.Z. Sun, B.Z. Tang, Efficient Solid Emitters with Aggregation-Induced Emission and Intramolecular Charge Transfer Characteristics: Molecular Design, Synthesis, Photophysical Behaviors, and OLED Application, *Chem. Mater.* 24 (2012) 1518–1528, <https://doi.org/10.1021/cm300416y>.
- [24] H. Li, Z. Chi, X. Zhang, B. Xu, S. Liu, Y. Zhang, J. Xu, New thermally stable aggregation-induced emission enhancement compounds for non-doped red organic light-emitting diodes, *Chem. Commun.* 47 (2011) 11273, <https://doi.org/10.1039/c1cc14642d>.
- [25] W.Z. Yuan, P. Lu, S. Chen, J.W.Y. Lam, Z. Wang, Y. Liu, H.S. Kwok, M. Yuguang, B.Z. Tang, Changing the behavior of chromophores from aggregation-caused quenching to aggregation-induced emission: Development of highly efficient light emitters in the solid state, *Adv. Mater.* 22 (2010) 2159–2163, <https://doi.org/10.1002/adma.200904056>.
- [26] Y. Li, J.-Y. Liu, Y.-D. Zhao, Y.-C. Cao, Recent advancements of high efficient donor-acceptor type blue small molecule applied for OLEDs, *Mater. Today* 20 (2017) 258–266, <https://doi.org/10.1016/j.mattod.2016.12.003>.
- [27] R. Balasaravanan, V. Sadhasivam, G. Sivaraman, A. Siva, Triphenylamino  $\alpha$ -Cyanovinyl- and Cyanoaryl-Based Fluorophores: Solvatochromism, Aggregation-Induced Emission and Electrochemical Properties, *Asian J. Org. Chem.* 5 (2016) 399–410, <https://doi.org/10.1002/ajoc.201500488>.
- [28] Z.Q. Yan, Z.Y. Yang, H. Wang, A.W. Li, L.P. Wang, H. Yang, B.R. Gao, Study of aggregation induced emission of cyano-substituted oligo (p-phenylenevinylene) by femtosecond time resolved fluorescence, *Spectrochim. Acta - Part A Mol. Biomol. Spectrosc.* 78 (2011) 1640–1645, <https://doi.org/10.1016/j.saa.2011.01.056>.
- [29] J. Liang, R.T.K. Kwok, H. Shi, B.Z. Tang, B. Liu, Fluorescent light-up probe with aggregation-induced emission characteristics for alkaline phosphatase sensing and activity study, *ACS Appl. Mater. Interfaces.* 5 (2013) 8784–8789, <https://doi.org/10.1021/am4026517>.
- [30] A. Singh, C.K. Lim, Y.D. Lee, J.H. Maeng, S. Lee, J. Koh, S. Kim, Tuning solid-state fluorescence to the near-infrared: A combinatorial approach to discovering molecular nanopores for biomedical imaging, *ACS Appl. Mater. Interfaces* 5 (2013) 8881–8888, <https://doi.org/10.1021/am4012066>.
- [31] M. Liu, P. Gao, Q. Wan, F. Deng, Y. Wei, X. Zhang, Recent advances and future prospects of aggregation-induced emission carbohydrate polymers, *Macromol. Rapid Commun.* 38 (2017) 1–11, <https://doi.org/10.1002/marc.201600575>.
- [32] M. Ipuy, Y.-Y. Liao, E. Jeanneau, P.L. Baldeck, Y. Bretonnière, C. Andraud, Solid state red biphotonic excited emission from small dipolar fluorophores, *J. Mater. Chem. C Mater. Opt. Electron. Devices* 4 (2016) 766–779, <https://doi.org/10.1039/C5TC03465E>.
- [33] X. Yang, X. Chen, X. Lu, C. Yan, Y. Xu, X. Hang, J. Qu, R. Liu, A highly selective and sensitive fluorescent chemosensor for detection of CN<sup>-</sup>, SO<sub>3</sub><sup>2-</sup> and Fe<sup>3+</sup> based on aggregation-induced emission, *J. Mater. Chem. C Mater. Opt. Electron. Devices* 4 (2016) 383–390, <https://doi.org/10.1039/C5TC02865E>.
- [34] V. Anand, B. Sadhasivam, R. Dhamodharan, Facile synthesis of triphenylamine and phenothiazine-based Schiff bases for aggregation-induced enhanced emission, white light generation, and highly selective and sensitive copper (< scp > ii < / scp >) sensing, *New J. Chem.* 42 (2018) 18979–18990, <https://doi.org/10.1039/C8NJ03316A>.
- [35] L. Basabe-Desmonts, D.N. Reinhoudt, M. Crego-Calama, Design of fluorescent materials for chemical sensing, *Chem. Soc. Rev.* 36 (2007) 993, <https://doi.org/10.1039/b609548h>.
- [36] S.K. Lanke, N. Sekar, Dyes and Pigments Aggregation induced emissive carbazole-based push pull NLOphores: synthesis, photophysical properties and DFT studies, *Dyes Pigm.* 124 (2016) 82–92, <https://doi.org/10.1016/j.dyepig.2015.09.013>.
- [37] B. Minaev, G. Baryshnikov, H. Agren, Principles of phosphorescent organic light emitting devices, *Phys. Chem. Chem. Phys.* 16 (2014) 1719–1758, <https://doi.org/10.1039/C3CP53806K>.
- [38] S. Xiao, Q. Cao, F. Dan, Solid-emissive BODIPY derivatives: design, synthesis and applications, *Curr. Org. Chem.* 16 (2012) 2970–2981, <https://doi.org/10.2174/138527212804546796>.
- [39] N. Wazzan, A. Irfan, Theoretical study of triphenylamine-based organic dyes with mono-, di-, and tri-anchoring groups for dye-sensitized solar cells, *Org. Electron.* 63 (2018) 328–342, <https://doi.org/10.1016/j.orgel.2018.09.039>.
- [40] C. Grivas, M. Pollnau, Organic solid-state integrated amplifiers and lasers, *Laser Photon. Rev.* 6 (2012) 419–462, <https://doi.org/10.1002/lpor.201100034>.
- [41] S. Redon, G. Eucat, M. Ipuy, E. Jeanneau, I. Gautier-Luneau, A. Ibanez, C. Andraud, Y. Bretonnière, Tuning the solid-state emission of small push-pull dipolar dyes to the far-red through variation of the electron-acceptor group, *Dyes Pigm.* 156 (2018) 116–132, <https://doi.org/10.1016/j.dyepig.2018.03.049>.
- [42] X. Hou, C. Ke, C.J. Bruns, P.R. McGonigal, R.B. Pettman, J.F. Stoddart, Tunable solid-state fluorescent materials for supramolecular encryption, *Nat. Commun.* 6 (2015) 6884, <https://doi.org/10.1038/ncomms7884>.
- [43] W.Z. Yuan, Y. Gong, S. Chen, X.Y. Shen, J.W.Y. Lam, P. Lu, Y. Lu, Z. Wang, R. Hu, N. Xie, H.S. Kwok, Y. Zhang, J.Z. Sun, B.Z. Tang, Efficient solid emitters with aggregation-induced emission and intramolecular charge transfer characteristics: molecular design, synthesis, photophysical behaviors, and OLED application, *Chem. Mater.* 24 (2012) 1518–1528, <https://doi.org/10.1021/cm300416y>.
- [44] S.P. Anthony, Organic solid-state fluorescence: strategies for generating switchable and tunable fluorescent materials, *ChemPlusChem* 77 (2012) 518–531, <https://doi.org/10.1002/cplu.201200073>.
- [45] V.D. Gupta, A.B. Tathe, V.S. Padalkar, P.G. Umape, N. Sekar, Red emitting solid state fluorescent triphenylamine dyes: synthesis, photo-physical property and DFT study, *Dyes Pigm.* 97 (2013) 429–439, <https://doi.org/10.1016/j.dyepig.2012.12.024>.
- [46] Y. Yang, B. Li, L. Zhang, Design and synthesis of triphenylamine-malonitrile derivatives as solvatochromic fluorescent dyes, *Sens. Actuators, B Chem.* 183 (2013) 46–51, <https://doi.org/10.1016/j.snb.2013.03.108>.
- [47] H. Wang, Y. Liu, M. Li, H. Huang, H.M. Xu, R.J. Hong, H. Shen, Multifunctional TiO<sub>2</sub> nanowires-modified nanoparticles bilayer film for 3D dye-sensitized solar cells, *Optoelectron. Adv. Mater. Rapid Commun.* 4 (2010) 1166–1169, <https://doi.org/10.1039/b000000x>.
- [48] S.P. Singh, M.S. Roy, K.R.J. Thomas, S. Balaiah, K. Khanuprakash, G.D. Sharma, New triphenylamine-based organic dyes with different numbers of anchoring groups for dye-sensitized solar cells, *J. Phys. Chem. C* 116 (2012) 5941–5950, <https://doi.org/10.1021/jp210971u>.
- [49] S.H. Kim, J. Choi, C. Sakong, J.W. Namgoong, W. Lee, D.H. Kim, B. Kim, M.J. Ko, J.P. Kim, The effect of the number, position, and shape of methoxy groups in triphenylamine donors on the performance of dye-sensitized solar cells, *Dyes Pigm.* 113 (2015) 390–401, <https://doi.org/10.1016/j.dyepig.2014.09.014>.
- [50] R. Kumari, A. Varghese, L. George, A. K.B. Photophysical study of 6-amino-3-methyl-4-(4-nitrophenyl)-1,4-dihydropyridano[2,3-*c*]pyrazole-5-carbonitrile and estimation of ground-state and singlet excited-state dipole moments by solvatochromic approaches, *J. Mol. Liq.* 222 (2016) 828–835, <https://doi.org/10.1016/j.molliq.2016.07.133>.
- [51] Y. Sun, X. Liang, Y. Zhao, J. Fan, Solvent effects on the absorption and fluorescence spectra of rhaponticin: experimental and theoretical studies, *Spectrochim. Acta Part A Mol. Biomol. Spectrosc.* 102 (2013) 194–199, <https://doi.org/10.1016/j.saa.2012.10.013>.
- [52] V.R. Desai, A.H. Sidarai, S.M. Hunagund, M. Basanagouda, R.M. Melavanki, R.H. Fattepur, J.S. Kadadevarmath, Steady state absorption and fluorescence study: estimation of ground and excited state dipole moments of newly synthesized pyridazin-3(2H)-one derivatives, *J. Mol. Liq.* 223 (2016) 141–149, <https://doi.org/10.1016/j.molliq.2016.08.015>.
- [53] B. Siddlingeshwar, S.M. Hanagodimath, E.M. Kirilova, G.K. Kirilov, Photophysical characteristics of three novel benzanthrone derivatives: experimental and theoretical estimation of dipole moments, *J. Quant. Spectrosc. Radiat. Transf.* 112 (2011) 448–456, <https://doi.org/10.1016/j.jqsrt.2010.09.001>.
- [54] G.V. Muddapur, V.V. Koppal, N.R. Patil, R.M. Melavanki, Photophysical properties of thiazidiazoles derivative: estimation of ground and excited state dipole moments by theoretical and experimental approach, *AIP Conf. Proc.* (2016), <https://doi.org/10.1063/1.4946424> p. 20373.
- [55] X. Gan, Y. Wang, X. Ge, W. Li, X. Zhang, W. Zhu, H. Zhou, J. Wu, Y. Tian, Triphenylamine isophorone derivatives with two photon absorption: photo-physical property, DFT study and bio-imaging, *Dyes Pigm.* 120 (2015) 65–73, <https://doi.org/10.1016/j.dyepig.2015.04.007>.

- [56] Y. Wang, Y. Jiang, D. Liu, Y. Wang, G. Wang, J. Hua, Ultrafast responses of two V-shaped compounds with a reverse conjugated structural configuration: an investigation of the reason for the enhanced two-photon absorption cross-section, *Appl. Phys. B* 124 (2018) 98, <https://doi.org/10.1007/s00340-018-6972-3>.
- [57] S. Kothavale, S. Katariya, N. Sekar, NLOphoric rigid pyrazino-phenanthroline donor- $\pi$ -acceptor compounds: investigation of structural and solvent effects on non-linear optical properties using computational methods, *Opt. Mater. (Amst.)* 75 (2018) 379–389, <https://doi.org/10.1016/j.optmat.2017.10.050>.
- [58] Y. Erande, S. Kothavale, M.C. Sreenath, S. Chitrambalam, I.H. Joe, N. Sekar, NLOphoric multichromophoric auxiliary methoxy aided triphenylamine D- $\pi$ -A chromophores – spectroscopic and computational studies, *Opt. Mater. (Amst.)* 73 (2017) 602–616, <https://doi.org/10.1016/j.optmat.2017.09.017>.
- [59] K.C. Avhad, D.S. Patil, Y.K. Gawale, S. Chitrambalam, M.C. Sreenath, I.H. Joe, N. Sekar, Large stokes shifted far-red to NIR-Emitting D- $\pi$ -A coumarins: combined synthesis, experimental, and computational investigation of spectroscopic and non-linear optical properties, *ChemistrySelect* 3 (2018) 4393–4405, <https://doi.org/10.1002/slct.201800063>.
- [60] Gaussian 09 Citation, (n.d.).
- [61] A.D. Becke, A new mixing of Hartree–Fock and local density-functional theories, *J. Chem. Phys.* 98 (1993) 1372, <https://doi.org/10.1063/1.464304>.
- [62] C. Lee, W. Yang, R.G. Parr, Development of the Colle-Salvetti correlation-energy formula into a functional of the electron density, *Phys. Rev. B* 37 (1988) 785–789, <https://doi.org/10.1103/PhysRevB.37.785>.
- [63] M. Rajeshirke, N. Sekar, NLO properties of ester containing fluorescent carbazole based styryl dyes – consolidated spectroscopic and DFT approach, *Opt. Mater. (Amst.)* 76 (2018) 191–209, <https://doi.org/10.1016/j.optmat.2017.12.035>.
- [64] U. Warde, N. Sekar, Solvatochromic benzo [h] coumarins: Synthesis, solvatochromism, NLO and DFT study, *Opt. Mater. (Amst.)* 72 (2017) 346–358, <https://doi.org/10.1016/j.optmat.2017.06.027>.
- [65] A. Abboto, L. Beverina, S. Bradamante, A. Facchetti, C. Klein, G.A. Pagani, M. Redi-Abshiro, R. Wortmann, A distinctive example of the cooperative interplay of structure and environment in tuning of intramolecular charge transfer in second-order nonlinear optical chromophores, *Chem. - A Eur. J.* 9 (2003) 1991–2007, <https://doi.org/10.1002/chem.200204356>.
- [66] C.R. Nayar, R. Ravikumar, Review: second order nonlinearities of Schiff bases derived from salicylaldehyde and their metal complexes, *J. Coord. Chem.* 67 (2014) 1–16, <https://doi.org/10.1080/00958972.2013.864759>.
- [67] S. Vidya, C. Ravikumar, I. Hubert Joe, P. Kumaradhas, B. Devipriya, K. Raju, Vibrational spectra and structural studies of nonlinear optical crystal ammonium D, L-tartrate: a density functional theoretical approach, *J. Raman Spectrosc.* 42 (2011) 676–684, <https://doi.org/10.1002/jrs.2743>.
- [68] M.J. Cho, S.K. Lee, J. Jin, D.H. Choi, L.R. Dalton, Electro-optic property of chromophore-terminated trifunctional dendrimer in a guest–host system, *Thin Solid Films* 515 (2006) 2303–2309, <https://doi.org/10.1016/j.tsf.2006.03.061>.